

## Mixing between $J_{\text{eff}} = \frac{1}{2}$ and $\frac{3}{2}$ orbitals in $\text{Na}_2\text{IrO}_3$ : A spectroscopic and density functional calculation study

C. H. Sohn,<sup>1,2</sup> H.-S. Kim,<sup>2</sup> T. F. Qi,<sup>3</sup> D. W. Jeong,<sup>1,2</sup> H. J. Park,<sup>1,2</sup> H. K. Yoo,<sup>1,2</sup> H. H. Kim,<sup>1</sup> J.-Y. Kim,<sup>4</sup> T. D. Kang,<sup>1,2</sup> Deok-Yong Cho,<sup>1,2</sup> G. Cao,<sup>3</sup> J. Yu,<sup>2</sup> S. J. Moon,<sup>5,\*</sup> and T. W. Noh<sup>1,2,†</sup>

<sup>1</sup>Center for Correlated Electron Systems, Institute for Basic Science, Seoul National University, Seoul 151-747, Korea

<sup>2</sup>Department of Physics and Astronomy, Seoul National University, Seoul 151-747, Korea

<sup>3</sup>Center for Advanced Materials, Department of Physics and Astronomy, University of Kentucky, Lexington, Kentucky 40506, USA

<sup>4</sup>Pohang Accelerator Laboratory, Pohang University of Science and Technology, Pohang 790-784, Korea

<sup>5</sup>Department of Physics, Hanyang University, Seoul 133-791, Korea

(Received 18 September 2012; revised manuscript received 20 July 2013; published 28 August 2013)

We investigated the electronic structure of  $\text{Na}_2\text{IrO}_3$  using optical spectroscopy, first-principles calculation, and x-ray absorption spectroscopy. We found that the electronic structure of  $\text{Na}_2\text{IrO}_3$  is mainly determined by anisotropic hopping interactions and spin-orbit coupling. Due to the hopping interaction, the orbital character of the bands near the Fermi level deviates from the spin-orbit coupling-induced  $J_{\text{eff}} = 1/2$  states. Polarization-dependent O 1s x-ray absorption spectroscopy showed that the  $J_{\text{eff}} = 1/2$  state of an Ir atom can be mixed with the  $J_{\text{eff}} = 3/2$  state of the neighboring Ir atom. This result implies that mixing between the  $J_{\text{eff}} = 1/2$  and  $3/2$  states in the valence state should be carefully considered in proposed exotic states of  $\text{Na}_2\text{IrO}_3$ , such as topological insulator and quantum spin liquid states.

DOI: [10.1103/PhysRevB.88.085125](https://doi.org/10.1103/PhysRevB.88.085125)

PACS number(s): 78.40.-q, 71.15.Mb, 78.20.-e, 78.70.Dm

Recently, iridates have received much attention as emergent materials for novel quantum phenomena, including spin-orbit coupling (SOC)-driven Mott transition or topological effects.<sup>1-9</sup> Most iridates have the  $\text{Ir}^{4+}$  valence state with  $t_{2g}^5$  electrons near the Fermi level,  $E_F$ , and the strong SOC transforms the  $t_{2g}^5$  states into the  $J(=L+S)$  states. The spin-orbital admixture can be represented with effective total angular momentum  $J_{\text{eff}} = 1/2$  and  $J_{\text{eff}} = 3/2$ , as observed in layered perovskite  $\text{Sr}_2\text{IrO}_4$ .<sup>1-3</sup> The  $J_{\text{eff}}$  quantum states of valence electrons will provide a new basis for understandings of  $5d$  transition metal oxides,<sup>4-14</sup> in which SOC is much stronger than in  $3d$  transition metal oxides.

$\text{Na}_2\text{IrO}_3$  is a particularly intriguing material whose  $J_{\text{eff}}$  states may lead to novel ground states.  $\text{Na}_2\text{IrO}_3$  has edge-sharing  $\text{IrO}_6$  octahedra that form a honeycomb lattice, where the exchange interaction between two Ir atoms can be highly anisotropic. Within the  $J_{\text{eff}}$  quantum state, it has been proposed that the magnetic ground state of  $\text{Na}_2\text{IrO}_3$  could be explained in terms of the Kitaev–Heisenberg model.<sup>5</sup> Many researchers have tried to identify quantum spin liquid,<sup>15-19</sup> one of the ground states of the Kitaev–Heisenberg model. In addition, the transfer integral between the next nearest neighboring Ir orbital via the oxygen orbitals is complex and spin dependent. This could induce a nonzero Berry phase, leading to a topologically nontrivial band structure in  $\text{Na}_2\text{IrO}_3$ .<sup>4,8</sup> It should be noted that the central presumption for the nontrivial ground states in  $\text{Na}_2\text{IrO}_3$  is the full occupation of four  $J_{\text{eff}} = 3/2$  states and single electron occupation in the  $J_{\text{eff}} = 1/2$  state.

However, the orbital characters of the valence bands of  $\text{Na}_2\text{IrO}_3$  have not been elucidated. Earlier theoretical work assumed the ideal  $J_{\text{eff}} = 1/2$  orbital in a cubic octahedron and suggested the nontrivial electric and magnetic ground states in  $\text{Na}_2\text{IrO}_3$ .<sup>4,5</sup> Later, detailed structural studies showed that Ir-O octahedra have a rather significant trigonal distortion, which makes the larger O-Ir-O bond angle about  $94.5^\circ$ .<sup>17,18</sup> Bhattacharjee *et al.* pointed out that the crystal field due to

the large trigonal distortion could destabilize the  $J_{\text{eff}} = 1/2$  states.<sup>20</sup> However, a recent resonant inelastic x-ray scattering experiment revealed that the trigonal crystal field is minimal; thus, the SOC-induced  $J_{\text{eff}} = 1/2$  orbital scenario is still valid in  $\text{Na}_2\text{IrO}_3$ .<sup>21</sup> On the other hand, Mazin *et al.* theorized that the pure  $J_{\text{eff}} = 1/2$  atomic-orbital scenario might not be valid in  $\text{Na}_2\text{IrO}_3$  due to the extended nature of the  $5d$  orbitals and the honeycomb structure.<sup>22</sup> They suggested that the highly anisotropic hopping interaction in the Ir-O-Ir network causes electrons to move only within a honeycomb composed of six Ir ions. This interaction results in quasimolecular orbitals, which are distinct from the pure  $J_{\text{eff}} = 1/2$  and  $3/2$  states. In these respects, it is important to identify the orbital character of the bands near  $E_F$  before we attempt to identify theoretically suggested nontrivial ground states in  $\text{Na}_2\text{IrO}_3$ .

In this paper, we investigate the effects of anisotropic hopping interactions and SOC on the electronic structure of  $\text{Na}_2\text{IrO}_3$  using optical spectroscopy, first-principles calculations, and x-ray absorption spectroscopy (XAS). We observed five clear  $d$ - $d$  transitions in optical conductivity,  $\sigma(\omega)$ , which can be understood in terms of the Ir  $t_{2g}$  state splitting due to the anisotropic hopping interaction and SOC. Our polarization-dependent O 1s XAS data provide experimental evidence that the orbital character of the valence bands of  $\text{Na}_2\text{IrO}_3$  is a mixture of  $J_{\text{eff}} = 1/2$  and  $3/2$  states.

High-quality single-crystal  $\text{Na}_2\text{IrO}_3$  was grown using a self-flux method from off-stoichiometric quantities of  $\text{IrO}_2$  and  $\text{Na}_2\text{CO}_3$ .<sup>18</sup> We measured the near-normal incident  $ab$ -plane reflectance spectrum,  $R(\omega)$ , in the energy region between 10 meV and 1 eV at room temperature, and determined the optical constants between 0.74 and 5 eV using spectroscopic ellipsometry. We obtained  $\sigma(\omega)$  using Kramers–Kronig analysis. We also measured transmission spectra,  $T(\omega)$ , of thin crystals in the energy region between 10 meV and 1 eV to see minute spectral features.<sup>23</sup> We performed the O 1s XAS experiment at the 2A beamline of the Pohang Light Source in

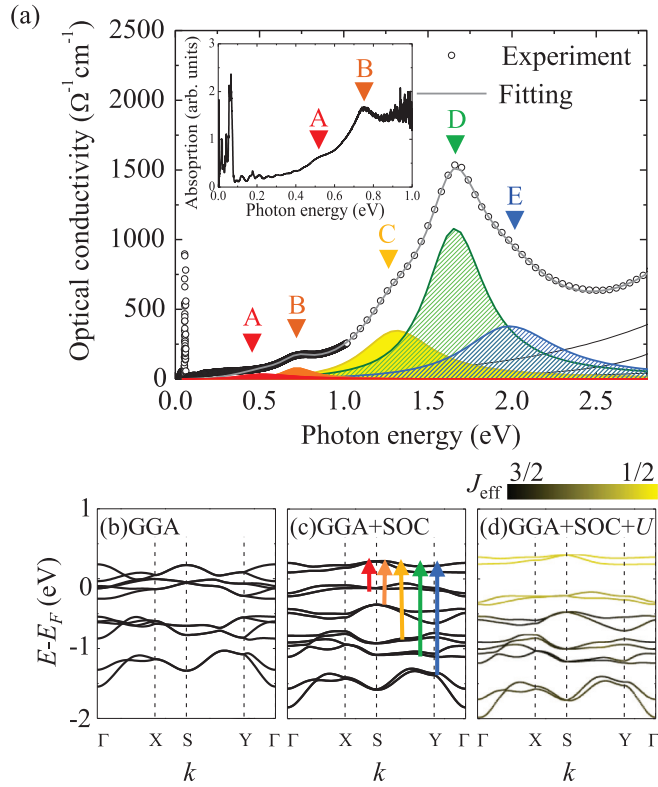


FIG. 1. (Color online) (a) Optical conductivity,  $\sigma(\omega)$ , of  $\text{Na}_2\text{IrO}_3$ . Black circles represent the experimental data, and the solid line is the Lorentz oscillator model fit. The inset of panel (a) shows absorption data below 1 eV. Results from DFT calculations: band structures of (b) GGA, (c) GGA + SOC, and (d) GGA + SOC +  $U$ . Each arrow in panel (c) indicates a possible optical interband transition between the  $t_{2g}$  orbital states. The yellow and black colors in panel (d) indicate the projected characters of the  $J_{\text{eff}} = 1/2$  and  $3/2$  orbitals, respectively.

the total electron yield mode. We calculated the band structure of  $\text{Na}_2\text{IrO}_3$  using a density functional theoretical (DFT) code, OpenMX,<sup>24</sup> which is based on the linear combination of pseudoatomic orbital formalism.<sup>25</sup> We used the Perdew–Burke–Ernzerhof generalized gradient approximation (GGA) function. Details of the calculation method have been reported elsewhere.<sup>26</sup>

Figure 1(a) displays  $\sigma(\omega)$  of  $\text{Na}_2\text{IrO}_3$ . We observe five peaks in  $\sigma(\omega)$  below 2.3 eV, which are marked using alphabetical symbols. Our conductivity data show two peaks below 1.0 eV (i.e., peaks A and B), which were not observed in the conductivity data of Ref. 27. These very weak spectral features can be seen more easily in  $T(\omega)$  than  $R(\omega)$ . As shown in the inset of Fig. 1(a), the absorption spectra obtained from  $T(\omega)$  clearly demonstrate the existence of peaks A and B. Because the charge-transfer excitations from the O  $2p$  to the Ir  $5d_{t_{2g}}$  states are located above 2.3 eV,<sup>27</sup> we can attribute all five peaks to the optical transitions between the Ir  $5d$  orbital states. To obtain more quantitative information on these low-energy  $d-d$  transitions, we fitted  $\sigma(\omega)$  with the Lorentz oscillator model,

$$\sigma(\omega) = \sum_n \frac{\omega^2 \gamma_n S_n}{(\omega_n^2 - \omega^2)^2 + \omega^2 \gamma_n^2} \quad (1)$$

TABLE I. Comparison of the energy values of the band gap and interband transitions ( $\omega_n$ ) estimated from the experimental  $\sigma(\omega)$  and theoretical band structure. The zigzag magnetic order found in inelastic neutron scattering experiments (Ref. 17) is employed in the band structure calculations. We note that nonmagnetic calculations of GGA+SOC do not produce band gaps, consistent with previous works (Refs. 22 and 27).

	Experiment	GGA + SOC	GGA + SOC + $U$
Band gap	0.32	0.05	0.28
A	0.52	0.30	0.53
B	0.72	0.67	0.86
C	1.32	1.05	1.22
D	1.66	1.24	1.39
E	1.98	1.65	1.88

where  $S_n$ ,  $\omega_n$ , and  $\gamma_n$  represent the strength, resonant frequency, and scattering rate of the  $n$ th oscillator, respectively. The results of the conductivity fitting are summarized in Table I.

The band dispersions from the GGA calculation are shown in Fig. 1(b). All of the calculated bands near  $E_F$  are very flat and located in three separate energy regions between  $-2$  and  $+0.5$  eV. These band dispersion features result from the formation of the quasimolecular orbital states, as pointed out by Mazin *et al.*<sup>22</sup> Namely, in the honeycomb lattice of  $\text{Na}_2\text{IrO}_3$ , the spatial orientations of the Ir  $5d_{t_{2g}}$  and O  $2p$  orbitals suppress the hopping in one particular direction at each Ir site. The direction of the highly anisotropic Ir-O-Ir hopping varies from one Ir site to another, which effectively causes electrons to move only in one hexagon, similar to the case of benzene. Such electron motion results in quasimolecular orbital states. Note that benzene has well-separated, flat energy levels with singlet, doublet, doublet, and singlet degeneracies.<sup>28</sup> According to Mazin *et al.*, the highly lying singlet and doublet states in  $\text{Na}_2\text{IrO}_3$  become degenerate due to the O-assisted next nearest neighbor hopping, resulting in three separate energy regions of bands.

The effects of the SOC on the electronic structure of  $\text{Na}_2\text{IrO}_3$  are illustrated in the result of the GGA + SOC calculation in Fig. 1(c). The SOC splits the energy levels from three to six well-separated energy regions. Note that in this band structure five  $d-d$  transitions between the  $t_{2g}$  orbitals are expected, as indicated by the arrows in Fig. 1(c). This is consistent with the experimentally observed five-peak structure in  $\sigma(\omega)$ . The quantitative agreement between the  $d-d$  transition energies of experiment and calculation can be achieved when the on-site Coulomb interaction  $U = 1.0$  eV is included [Fig. 1(d)]. As shown in Table I, the GGA + SOC +  $U$  calculation produced  $d-d$  transition energies that matched well with the experimental values. These calculation results demonstrate that the five distinct  $d-d$  transitions in our  $\sigma(\omega)$  data can be understood in terms of the combined effect of the formation of the quasimolecular orbital states and SOC in the honeycomb lattice of  $\text{Na}_2\text{IrO}_3$ .

The colors in Fig. 1(d) indicate the projection of the GGA + SOC +  $U$  calculation results to  $J_{\text{eff}} = 1/2$  (yellow color) and  $3/2$  (black color) orbitals. One can see that the states near the  $E_F$  have orbital characters close to the

$J_{\text{eff}} = 1/2$  state, and the others exhibit characters close to the  $J_{\text{eff}} = 3/2$  state. However, our calculation shows that there should be considerable mixing between  $J_{\text{eff}} = 1/2$  and  $3/2$  orbitals in every band. For example, unoccupied states and topmost-occupied states near  $E_F$  have  $J_{\text{eff}} = 3/2$  projections of about 14% and 30%, respectively. Such orbital mixings could be important for investigations of numerous proposed novel ground states of  $\text{Na}_2\text{IrO}_3$ .

To better understand the orbital characters of the bands near the  $E_F$ , we performed O 1s XAS. The O 1s XAS reflects the transition from the O 1s core level to the unoccupied O 2p states that are hybridized with the Ir 5d orbitals. Because the Ir 5d orbitals can hybridize with the surrounding 2p waves of six oxygen ions only when their point symmetries coincide, we can obtain information on the Ir 5d orbital characters using polarization-dependent XAS.<sup>29</sup> Figure 2(a) shows the experimental geometry. We fixed the incident angle of light at  $70^\circ$  and changed the light polarization to circumvent any saturation effects of the signals. The peak intensities reflect the directional O 2p–Ir 5d hybridization strengths.<sup>30</sup> Namely, the  $\sigma$ -polarized light probed (O  $2p_{x',y'}$ –Ir 5d), which corresponds to the density of the empty O  $2p_{x',y'}$  state hybridized with Ir 5d orbitals. On the other hand, the  $\pi$ -polarized light probed  $\sin^2 70^\circ$  (O  $2p'_z$ –Ir 5d) +  $\cos^2 70^\circ$  (O  $2p_{x',y'}$ –Ir 5d). The primed coordinates  $z'$  ( $x'$  and  $y'$ ) are perpendicular (parallel) to the Ir honeycomb plane, and the  $x$ ,  $y$ , and  $z$  coordinates are along the undistorted Ir-O direction, as displayed in Fig. 2(a).

Figure 2(b) shows the polarization-dependent O 1s XAS data for  $\text{Na}_2\text{IrO}_3$ . Three main peaks, labeled  $\alpha$ ,  $\beta$ , and  $\gamma$ , are

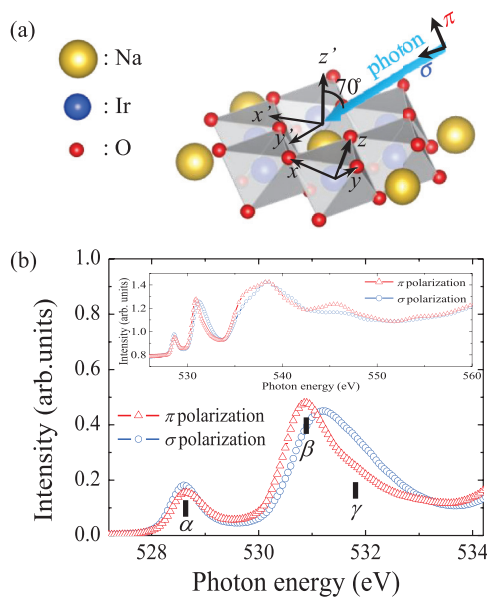


FIG. 2. (Color online) (a) Experimental geometry of polarization-dependent O 1s XAS. The primed coordinate  $z'$  ( $x'$ ,  $y'$ ) is perpendicular (parallel) to the Ir honeycomb plane, and  $x$ ,  $y$ , and  $z$  are along the undistorted Ir-O direction.  $\sigma$  polarization is parallel to the Ir honeycomb plane, and  $\pi$  polarization is perpendicular to both incident photon direction and  $\sigma$  polarization. (b) Polarization-dependent O 1s XAS data. Red triangles and blue circles represent  $\pi$  polarization and  $\sigma$  polarization data, respectively. The inset of panel (b) shows O 1s XAS raw data in broad energy region.

located at 528.7, 530.8, and 531.5 eV, respectively. Because the features are broad, possible chemical shifts in the O 1s core hole energy can be neglected. Peak  $\alpha$  can be attributed to the unoccupied  $t_{2g}$  orbital states, and peaks  $\beta$  and  $\gamma$  are due to the unoccupied  $e_g$  states. It is interesting to note that whereas the peaks related to  $e_g$  states ( $\beta$  and  $\gamma$ ) show polarization dependence as well as sizable splitting, the peak associated with  $t_{2g}$  states ( $\alpha$ ) exhibits negligible polarization dependence.

To obtain insight into the orbital character of the  $t_{2g}$  state, we first considered the polarization dependence of peaks  $\beta$  and  $\gamma$ , coming from  $e_g$  states. As shown in Fig. 2(b), peak  $\beta$  ( $\gamma$ ) is stronger in out-of-plane (in-plane) polarization. The energy splitting of  $e_g$  orbitals and their polarization dependence cannot be explained based on local interactions. The SOC cannot result in energy splitting and polarization dependences of the  $e_g$  orbital states, because the  $e_g$  orbital states are insensitive to SOC. The local trigonal distortion cannot explain the energy splitting of the  $e_g$  states, either, because  $e_g$  states provide a good basis for trigonal symmetry. Thus, the energy splitting and polarization dependence of these two peaks implies that a nonlocal interaction affects the orbital character of  $\text{Na}_2\text{IrO}_3$  significantly.

Now we consider peak  $\alpha$ , which exhibits little polarization dependence. The intensity ratio of peak  $\alpha$  in  $\pi$  and  $\sigma$  polarizations is estimated to be  $0.88 \pm 0.07$ . For comparison, we evaluated the intensity ratio in  $\pi$  and  $\sigma$  polarizations for the pure  $J_{\text{eff}} = 1/2$  orbital states. We calculated the hybridization between pure atomic  $J_{\text{eff}} = 1/2$  orbitals and O 2p orbitals with the inclusion of the reported value of the trigonal structural distortion in  $\text{Na}_2\text{IrO}_3$ .<sup>18</sup> We found that the intensity ratio  $\pi/\sigma$  should be 1.6 for the highly distorted  $\text{IrO}_6$  cluster.<sup>31</sup> This value is higher than the experimental value of  $0.88 \pm 0.07$ . Therefore, the negligible polarization dependence of peak  $\alpha$  indicates that the real orbital character of the unoccupied  $t_{2g}$  state should differ from that of the pure atomic  $J_{\text{eff}} = 1/2$  orbital.

To explain the deviation of the orbital character of the  $t_{2g}$  states from the  $J_{\text{eff}} = 1/2$  orbital, we considered the anisotropic hopping interaction.<sup>22</sup> The left side of Fig. 3(a) shows the Ir honeycomb net structure of  $\text{Na}_2\text{IrO}_3$ . The arrows on the right side of Fig. 3(a) indicate the dominant hopping processes in the Ir 5d in honeycomb structure between two nearest neighboring Ir atoms via O 2p orbitals. Electrons in the  $d_{yz}$  ( $d_{zx}$ ) orbital at one Ir site can hop to the  $d_{zx}$  ( $d_{yz}$ ) orbital of another Ir site via O  $2p_z$ , while electrons in the  $d_{xy}$  orbital at one Ir site cannot hop to any orbital at another Ir site via O  $2p_z$ . Due to this anisotropic intersite hopping process, the  $J_{\text{eff}} = 1/2$  state ( $\mp \frac{1}{\sqrt{3}}[|d_{xy}, \pm 1/2\rangle \pm |d_{yz}, \mp 1/2\rangle + i|d_{zx}, \mp 1/2\rangle]$ ) can be mixed with the  $J_{\text{eff}} = 3/2$  orbital ( $\mp \frac{1}{\sqrt{2}}[\pm |d_{zx}, \mp 1/2\rangle + i|d_{yz}, \mp 1/2\rangle]$ ). In the same way, the  $J_{\text{eff}} = 1/2$  state can be mixed with other  $J_{\text{eff}} = 3/2$  states,  $\mp \frac{1}{\sqrt{2}}[|d_{zx}, \pm 1/2\rangle + i|d_{xy}, \mp 1/2\rangle]$  and  $\mp \frac{1}{\sqrt{2}}[|d_{yz}, \pm 1/2\rangle \pm |d_{xy}, \mp 1/2\rangle]$ , via O  $2p_x$  and  $2p_y$ , respectively.

The mixed  $J_{\text{eff}} = 1/2$  and  $3/2$  states explain the small polarization dependence of peak  $\alpha$  in our XAS data. Due to the hybridization discussed above, the wavefunction of electrons of Ir ions can be written as  $\Psi = \sqrt{1 - |A|^2}|J_{\text{eff}} = 1/2\rangle - A|J_{\text{eff}} = 3/2\rangle$ , where  $A$  is a complex mixing coefficient. Using this wavefunction, we calculated the  $\pi/\sigma$  intensity ratio with

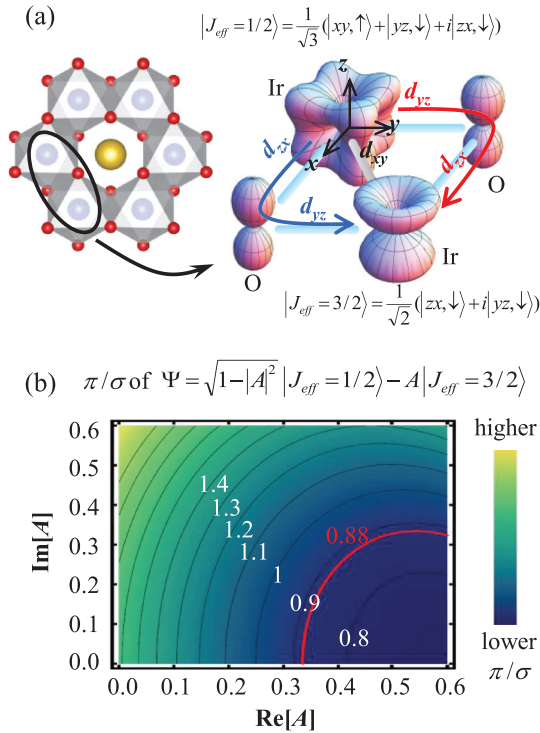


FIG. 3. (Color online) (a) Schematic diagram of the hopping process in  $\text{Na}_2\text{IrO}_3$ . The left side of panel (a) shows the Ir honeycomb net structure in  $\text{Na}_2\text{IrO}_3$ . For simplicity, we only show the hopping process in the region surrounded by the black circle, which contains two Ir atoms. Blue and red arrows indicate the dominant hopping process in rectangular Ir-O-Ir chains. (b) Calculated peak intensity ratio,  $\pi/\sigma$ , in O  $1s$  XAS data for distorted  $\text{IrO}_6$  octahedra as a function of the portion of  $J_{\text{eff}} = 3/2$  in the ground state of  $\Psi = \sqrt{1 - |A|^2}|J_{\text{eff}} = 1/2\rangle - A|J_{\text{eff}} = 3/2\rangle$ , where  $A = \text{Re}[A] + i\text{Im}[A]$  is the complex mixing coefficient. The black lines are contour plots for given values of  $\pi/\sigma$ , and corresponding values are shown in white. The experimental  $\pi/\sigma$  ratio of 0.88 is shown with the red line.

the variation in  $A = \text{Re}[A] + i\text{Im}[A]$  [Fig. 3(b)]. The black lines in Fig. 3(b) are contour plots for given values of  $\pi/\sigma$ . For the pure  $J_{\text{eff}} = 1/2$  orbital limit ( $A = 0$ ),  $\pi/\sigma$  is about 1.6. As  $|A|$  increases,  $\pi/\sigma$  decreases; namely, as mixing of the  $J_{\text{eff}} = 1/2$  and  $3/2$  states increases, polarization dependence decreases. Using the experimental value  $\pi/\sigma = 0.88$ , the minimum and maximum value of  $|A|^2$  was estimated to be

approximately 0.10 and 0.62, respectively. Thus, the portion of the  $J_{\text{eff}} = 3/2$  orbital in the unoccupied Ir  $5d$  state near the  $E_F$  is at least 10%, indicating considerable mixing between the  $J_{\text{eff}} = 1/2$  and  $3/2$  states. Whereas we cannot determine the exact value of  $|A|^2$  solely from the XAS data, weak strength of the peaks A and B in optical conductivity spectra [Fig. 1(a)] further supports that the orbital character should be close to the minimum value of  $|A|^2$ .<sup>32</sup> In addition, the minimum value of  $|A|^2$  is in good agreement with the theoretical estimation for unoccupied states (14%), as mentioned above [Fig. 1(d)].

The observation of sizable mixing between  $J_{\text{eff}} = 1/2$  and  $3/2$  orbitals implies that localized  $S = 1/2$  (pseudospin, in that case) Hamiltonian might not be appropriate to account for the ground states of  $\text{Na}_2\text{IrO}_3$ . Most of proposed theoretical models that predict exotic ground states of  $\text{Na}_2\text{IrO}_3$  assumed the full-filled  $J_{\text{eff}} = 3/2$  orbital and half-filled  $J_{\text{eff}} = 1/2$  orbital.<sup>4,5</sup> Under this circumstance, we can construct  $S = 1/2$  Hamiltonian, similar to the  $3d$  transition metal oxides system. However, our experimental results clearly showed that the orbital character of  $\text{Na}_2\text{IrO}_3$  deviates from the localized  $J_{\text{eff}} = 1/2$  orbital. Instead, as Mazin *et al.* pointed out,<sup>22</sup> our XAS data indicated the delocalized nature of electrons in  $\text{Na}_2\text{IrO}_3$ . Therefore, we insist that  $S = 1/2$  Hamiltonian needs to be modified to understand the orbital and magnetic ground state of  $\text{Na}_2\text{IrO}_3$ .

In conclusion, we found that the anisotropic hopping interaction in the honeycomb Ir lattice contributes to  $J$ -state mixing in  $\text{Na}_2\text{IrO}_3$ . Along with the strong SOC effect,  $J$ -state mixing explains the experimental observations of the five  $d$ - $d$  transitions in optical conductivity and the negligible polarization dependence of the  $t_{2g}$  peak in the XAS spectra. These findings suggest that the mixed nature of the  $J_{\text{eff}} = 1/2$  and  $3/2$  states should be taken into account in future studies of novel ground states of  $\text{Na}_2\text{IrO}_3$ .

This work was supported by the Institute for Basic Science (IBS) in Korea. S.J.M. was supported by Basic Science Research Program through the National Research Foundation of Korea funded by the Ministry of Science, ICT & Future Planning (2012R1A1A1013274). J.Y. and H.S.K. were supported by the NRF through the ARP (R17-2008-033-01000-0). The work at the University of Kentucky was supported by NSF through grants DMR-0856234 and EPS-0814194. Experiments at Pohang Light Source were supported by MEST and POSTECH.

\*soonjmoon@hanyang.ac.kr

†twnoh@snu.ac.kr

<sup>1</sup>B. J. Kim, Hosub Jin, S. J. Moon, J.-Y. Kim, B.-G. Park, C. S. Leem, Jaejun Yu, T. W. Noh, C. Kim, S.-J. Oh, J.-H. Park, V. Durairaj, G. Cao, and E. Rotenberg, *Phys. Rev. Lett.* **101**, 076402 (2008).

<sup>2</sup>S. J. Moon, H. Jin, K. W. Kim, W. S. Choi, Y. S. Lee, J. Yu, G. Cao, A. Sumi, H. Funakubo, C. Bernhard, and T. W. Noh, *Phys. Rev. Lett.* **101**, 226402 (2008).

<sup>3</sup>B. J. Kim, H. Ohsumi, T. Komesu, S. Sakai, T. Morita, H. Takagi, and T. Arima, *Science* **323**, 1329 (2009).

<sup>4</sup>A. Shitade, H. Katsura, J. Kuneš, X.-L. Qi, S.-C. Zhang, and N. Nagaosa, *Phys. Rev. Lett.* **102**, 256403 (2009).

<sup>5</sup>J. Chaloupka, G. Jackeli, and G. Khaliullin, *Phys. Rev. Lett.* **105**, 027204 (2010).

<sup>6</sup>K. Ishii, I. Jarrige, M. Yoshida, K. Ikeuchi, J. Mizuki, K. Ohashi, T. Takayama, J. Matsuno, and H. Takagi, *Phys. Rev. B* **83**, 115121 (2011).

<sup>7</sup>I. Kimchi and Y.-Z. You, *Phys. Rev. B* **84**, 180407 (2011).

<sup>8</sup>C. H. Kim, H. S. Kim, H. Jeong, H. Jin, and J. Yu, *Phys. Rev. Lett.* **108**, 106401 (2012).

<sup>9</sup>Y. Singh, S. Manni, J. Reuther, T. Berlijn, R. Thomale, W. Ku, S. Trebst, and P. Gegenwart, *Phys. Rev. Lett.* **108**, 127203 (2012).

<sup>10</sup>D. Pesin and L. Balents, *Nature Physics* **6**, 376 (2010).

<sup>11</sup>B.-J. Yang and Y. B. Kim, *Phys. Rev. B* **82**, 085111 (2010).

- <sup>12</sup>X. Wan, A. M. Turner, A. Vishwanath, and S. Y. Savrasov, *Phys. Rev. B* **83**, 205101 (2011).
- <sup>13</sup>A. Go, W. Witczak-Krempa, G. S. Jeon, K. Park, and Y. B. Kim, *Phys. Rev. Lett.* **109**, 066401 (2012).
- <sup>14</sup>W. Witczak-Krempa and Y. B. Kim, *Phys. Rev. B* **85**, 045124 (2012).
- <sup>15</sup>Y. Singh and P. Gegenwart, *Phys. Rev. B* **82**, 064412 (2010).
- <sup>16</sup>X. Liu, T. Berlijn, W. G. Yin, W. Ku, A. Tsvelik, Y.-J. Kim, H. Gretarsson, Y. Singh, P. Gegenwart, and J. P. Hill, *Phys. Rev. B* **83**, 220403 (2011).
- <sup>17</sup>S. K. Choi, R. Coldea, A. N. Kolmogorov, T. Lancaster, I. I. Mazin, S. J. Blundell, P. G. Radaelli, Yogesh Singh, P. Gegenwart, K. R. Choi, S.-W. Cheong, P. J. Baker, C. Stock, and J. Taylor, *Phys. Rev. Lett.* **108**, 127204 (2012).
- <sup>18</sup>F. Ye, S. Chi, H. Cao, B. C. Chakoumakos, J. A. Fernandez-Baca, R. Custelcean, T. F. Qi, O. B. Korneta, and G. Cao, *Phys. Rev. B* **85**, 180403 (2012).
- <sup>19</sup>J. Chaloupka, G. Jackeli, and G. Khaliullin, *Phys. Rev. Lett.* **110**, 097204 (2013).
- <sup>20</sup>S. Bhattacharjee, S. S. Lee, and Y. B. Kim, *New J. Phys.* **14**, 073015 (2012).
- <sup>21</sup>H. Gretarsson, J. P. Clancy, X. Liu, J. P. Hill, E. Bozin, Y. Singh, S. Manni, P. Gegenwart, J. Kim, A. H. Said, D. Casa, T. Gog, M. H. Upton, H. S. Kim, J. Yu, V. M. Katukuri, L. Hozoi, J. van den Brink, and Y. J. Kim, *Phys. Rev. Lett.* **110**, 076402 (2013).
- <sup>22</sup>I. I. Mazin, H. O. Jeschke, K. Foyevtsova, R. Valentí, and D. I. Khomskii, *Phys. Rev. Lett.* **109**, 197201 (2012).
- <sup>23</sup>H. S. Choi, Y. S. Lee, T. W. Noh, E. J. Choi, Y. Bang, and Y. J. Kim, *Phys. Rev. B* **60**, 4646 (1999).
- <sup>24</sup>The DFT code, OpenMX, is available at the web site (<http://www.openmx-square.org>) released under the GNU General Public License.
- <sup>25</sup>T. Ozaki, *Phys. Rev. B* **67**, 155108 (2003).
- <sup>26</sup>H.-S. Kim, C. H. Kim, H. Jeong, H. Jin, and J. Yu, *Phys. Rev. B* **87**, 165117 (2013).
- <sup>27</sup>R. Comin, G. Levy, B. Ludbrook, Z.-H. Zhu, C. N. Veenstra, J. A. Rosen, Yogesh Singh, P. Gegenwart, D. Stricker, J. N. Hancock, D. van der Marel, I. S. Elfimov, and A. Damascelli, *Phys. Rev. Lett.* **109**, 266406 (2012).
- <sup>28</sup>M. S. Dresselhaus, G. Dresselhaus, and A. Jorio, *Group Theory: Application to the Physics of Condensed Matter* (Springer, Berlin, Heidelberg, Germany, 2008), Sec. 7.5.3.
- <sup>29</sup>W. B. Wu, D. J. Huang, J. Okamoto, A. Tanaka, H. J. Lin, F. C. Chou, A. Fujimori, and C. T. Chen, *Phys. Rev. Lett.* **94**, 146402 (2005).
- <sup>30</sup>J. C. Slater and G. F. Koster, *Phys. Rev.* **94**, 1498 (1954).
- <sup>31</sup>We only considered trigonal distortion itself and ignored the effects of the trigonal crystal field because there is theoretical and experimental evidence of a small trigonal crystal field in  $\text{Na}_2\text{IrO}_3$ .<sup>21,22</sup>
- <sup>32</sup>The optical  $d-d$  transition can be understood as an electron hopping from one Ir site to another Ir site via O  $2p$  orbitals. Because the Ir-O-Ir angle is close to  $90^\circ$  in  $\text{Na}_2\text{IrO}_3$ , hopping between the  $J_{\text{eff}} = 1/2$  orbital states of the nearest neighbors is strongly suppressed. Therefore, the weak strength of peaks A and B in optical conductivity [Fig. 1(a)] implies that the contribution of the  $J_{\text{eff}} = 1/2$  orbital to states near the  $E_F$  is much stronger than that of the  $J_{\text{eff}} = 3/2$  orbital.